Isospin effect in $\pi^{\pm}$ ^{14}C elastic scattering at 50 MeV

C. S. Mishra, B. M. Preedom, B. G. Ritchie,* and R. S. Moore
University of South Carolina, Columbia, South Carolina 29208

M. Blecher and K. Gotow
Virginia Polytechnic Institute and State University, Blacksburg, Virginia 24061

R. L. Burman, M. V. Hynes, and E. Piasetzky
Los Alamos National Laboratory, Los Alamos, New Mexico 87545

N. S. Chant and P. G. Roos
University of Maryland, College Park, Maryland 20742

F. E. Bertrand, T. Sjoreen, F. E. Obenshain, and E. E. Gross
Oak Ridge National Laboratory, Oak Ridge, Tennessee 37830
(Received 23 May 1985)

Angular distributions have been measured for $\pi^{\pm}$ elastic scattering at 50 MeV from ^{14}C. Comparison with previously measured distributions for ^{12}C shows a significant isotopic difference for π^{-} scattering. The data were analyzed using the second order Michigan State University optical potential proposed for low energy pion nucleus elastic scattering. Agreement with the data was obtained using the same density distributions for the protons and neutrons.

I. INTRODUCTION

Angular distributions for low energy ($T_{\pi} \leq 80$ MeV) elastic scattering of $\pi^{\pm}$ on several nuclei[1-3] have been measured and partially summarized in reviews.[4] Previous measurements concentrated on $N=Z$, $T=0$ nuclei, or nuclei which had single or double closed shells. The measurements presented here are for elastic scattering of 50 MeV $\pi^{\pm}$ from the $T=1$ nucleus ^{14}C. This study complements work performed on the same nucleus at 65 and 80 MeV.[5]

The present $\pi^{\pm}$ cross sections for ^{14}C and previously published ^{12}C cross sections[2,6] are compared with calculations which use the second order Michigan State University (MSU) (Refs. 7 and 8) optical potential. The MSU potential explicitly contains terms proportional to the neutron-proton density difference in both first and second order. This model describes reasonably well the angular distributions of 20 to 50 MeV pion elastic scattering over the range of nuclei from ^{12}C to ^{208}Pb. As shown here, the MSU potential can be used to describe the measured angular distributions of $\pi^{\pm}$ elastic scattering from ^{14}C.

II. EXPERIMENTAL PROCEDURE

This experiment was performed at the Clinton P. Anderson Meson Physics Facility (LAMPF), using the low energy pion (LEP) channel and the Bicentennial spectrometer as discussed in detail in previous publications.[3,9] The salient features of the experimental method are reviewed here. The beam was aligned on the target by using a multiwire profile monitor. The beam size on the target was 0.3 cm$\times$1.0 cm (FWHM). The momentum resolution of the beam was $\Delta P/P=1.0\%$, except at the forward angles where $\Delta P/P=0.25\%$. The pion energy at the center of the target was 50.1 MeV.

The ^{14}C target, in powder form, was contained in a stainless steel envelope of 0.0025 cm thickness. The ^{12}C contamination (21.7$\pm$1.7)% (Ref. 10) was used to measure the thickness of the target by comparing the excitation of the 4.44 MeV state of ^{12}C in the ^{14}C target with the excitation of the same state from a pressed ^{12}C target. The areal density of the ^{14}C target was thus measured to be 0.11$\pm$0.01 g/cm^2. For each setting of the spectrometer and the channel, scattering from an identical, empty stainless steel envelope was measured with sufficient statistics to correct for the background due to stainless steel.

An overall resolution of $\sim$1.25 MeV (FWHM) was obtained. Since this resolution was not sufficient to separate the elastic scattering peak from the stainless steel, a background subtraction was made from the total carbon plus steel spectra. The laboratory differential cross section for carbon, corrected for the stainless steel background, was obtained by the relation

$$\left[\frac{d\sigma}{d\Omega}\right]_{\text{lab}} = \frac{N_{\text{el}} A \cos\theta_t}{N_{\pi\mu}\rho t N_A \alpha} ,$$

where N_{el} is the number of counts in the elastic peak due to ^{14}C and the ^{12}C contamination, θ_t is the target angle, $N_{\pi\mu}$ is the number of counts in the relative monitor, α is the absolute normalization factor, N_A is Avogadro's number, and ρ, t, and A are the target density, thickness, and atomic mass, respectively. The normalization factor, α, included the effective solid angle of the spectrometer, pion decay in the spectrometer, the efficiency of the detection

TABLE I. Elastic differential cross sections for $^{14}C(\pi^{\pm},\pi^{\pm})^{14}C$ at 50 MeV. Scattering angles and cross sections are in center of mass with units of deg and mb/sr, respectively. The pion energy at the center of the target was 50.1 MeV.

	π^+		π^-	
$\theta_{c.m.}$	$(d\sigma/d\Omega)_{c.m.}$	$\Delta\sigma_{c.m.}$[a]	$(d\sigma/d\Omega)_{c.m.}$	$\Delta\sigma_{c.m.}$[a]
30.4	15.06	1.34		
40.5	10.30	0.84	26.68	1.91
50.6	5.54	0.42	8.79	1.40
60.7	3.30	0.27	3.86	0.46
70.8	2.97	0.23	5.35	0.40
80.8	4.61	0.25	8.30	0.43
90.8	5.66	0.24	10.42	0.46
100.8	6.17	0.30	10.71	0.49
110.8	6.85	0.32	10.12	0.42
120.7	5.66	0.30	9.18	0.41

[a]The errors shown are due to statistics. The normalization error which includes the error in the target density is 10.5% for π^+ and 12.5% for π^-. The normalization error, excluding the target density error, is 3.7% for π^+ and 5.5% for π^-.

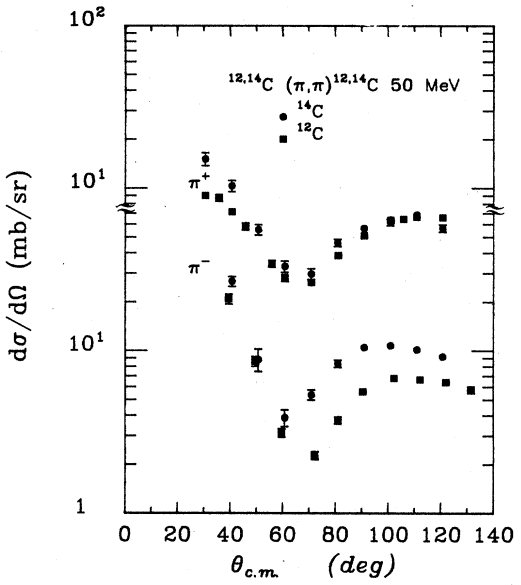

FIG. 1. Elastic differential cross sections for $\pi^{\pm}$ scattering on ^{14}C and ^{12}C at 50 MeV. For ^{12}C, the π^+ data are from Ref. 2 and the π^- data are from Ref. 6.

system, and the number of pions incident on the target relative to the pion decay monitor telescope.

To obtain the elastic scattering cross section for ^{14}C it was necessary to subtract the contribution due to scattering from the ^{12}C contamination. Since ^{12}C elastic scattering cross sections have been measured previously,[2,6] such a subtraction could be made directly by using the relation

$$\left[\frac{d\sigma}{d\Omega}\right]_{^{14}C}=\left[\frac{d\sigma}{d\Omega}\right]_{^{14}C+^{12}C}-(0.217\pm0.017)\left[\frac{d\sigma}{d\Omega}\right]_{^{12}C}.$$

The relative normalization was accomplished with a pion decay monitor telescope[11] placed at an angle within the Jacobian peak angle. This setting kept the monitor insensitive to shifts in beam centroid and the position and angle of the spectrometer. The absolute normalization was determined by measuring π^+p elastic scattering at $\theta_{lab}=95°$ from a CH_2 target ($\rho t=0.236$ g/cm^2) and normalizing to the measurement[12] of Bertin *et al.* at 50 MeV. No accurate values for π^-p elastic scattering existed in the literature. Thus for the π^- normalization we used the calibration of the relative monitor obtained for π^+. We kept the geometrical configuration of the channel fixed and ensured that the π^- beam spot was the same as that for π^+, to keep the phase space nearly identical. The normalization errors in the π^- cross sections were increased as indicated in Table I to account for our estimate of the small differences in geometry.

III. RESULTS AND ANALYSIS

The ^{14}C differential cross sections are listed in Table I and are shown in Fig. 1 together with the ^{12}C angular distributions. The first minimum ($\sim65°$) in the angular distribution results from the interference between the repulsive πN s-wave and the attractive πN p-wave amplitudes. A significant difference in the differential cross section is observed between $^{14}C(\pi^-,\pi^-)^{14}C$ and $^{12}C(\pi^-,\pi^-)^{12}C$ at back angles, where the ^{14}C cross section is approximately a factor of 2 larger than ^{12}C. The minimum of the s-p wave interference is shifted towards smaller angles by $\sim10°$ for ^{14}C relative to ^{12}C for π^- and the ^{14}C cross section at the minimum is larger. These effects can be interpreted as indicating a stronger p-wave attraction due to the two additional neutrons in ^{14}C. The $^{14}C(\pi^+,\pi^+)^{14}C$ cross section is similar to the $^{12}C(\pi^+,\pi^+)^{12}C$ cross section except at small angles, where the ^{14}C cross sections are larger than for ^{12}C. The sensitivity of the pion interaction with the excess neutrons increases as the pion energy decreases from 80 to 50 MeV. This neutron density effect is larger for 50 MeV π^- scattering than 80 MeV π^- scattering, as shown in Fig. 2.

The striking difference between the ^{14}C and ^{12}C angular distributions for the two probes offers a useful test of reaction models. Optical model calculations using the second order MSU potential[7,8] were performed for the angular distributions presented in Fig. 1.

The MSU optical potential consists of both isoscalar and isovector interactions with second order terms which take into account πNN effects, Pauli blocking, the Lorentz-Lorenz-Ericson-Ericson (LLEE) effect, true absorption, angle transformation, Fermi averaging, nuclear binding, and other terms.

The MSU optical potential used for the calculation presented here has the form

$$\begin{aligned}2\bar{\omega}U_{opt}=&-4\pi[b(r)+B(r)]\\&+4\pi\nabla\cdot\{L(r)[c(r)+C(r)]\}\nabla\\&-4\pi\left[\frac{p_1-1}{2}\nabla^2c(r)+\frac{p_2-1}{2}\nabla^2C(r)\right]\\&+2\bar{\omega}V_c(r),\end{aligned}$$

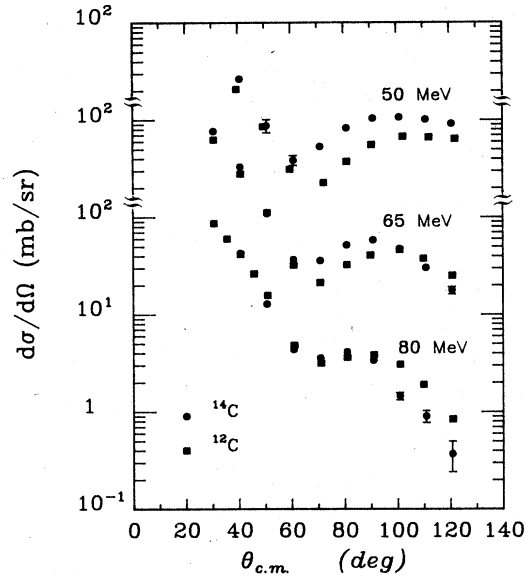

FIG. 2. Comparison of $^{14}C(\pi^-,\pi^-)^{14}C$ and $^{12}C(\pi^-,\pi^-)^{12}C$ cross sections at 80, 65, and 50 MeV. The 80 and 65 MeV data are from Ref. 5.

where

$$b(r)=p_1[\bar{b}_0\rho(r)-q_\pi b_1\delta\rho(r)] ,$$

$$c(r)=\frac{1}{p_1}[c_0\rho(r)-q_\pi c_1\delta\rho(r)] ,$$

$$B(r)=p_2B_0\rho^2(r) ,$$

$$C(r)=\frac{1}{p_2}C_0\rho^2(r) ,$$

$$L(r)=\left\{1+\frac{4\pi}{3}[c(r)+C(r)]\right\}^{-1} ,$$

$$\bar{b}_0\simeq b_0-\frac{3}{2\pi}(b_0^2+2b_1^2)K_F ,$$

$$\bar{\omega}=\omega/(1+\epsilon/A) ,$$

$$\epsilon=\omega/M ,$$

$$M=(\text{nuclear mass})/A\cong 931 \text{ MeV} .$$

The subscripts zero and one refer to isoscalar and isovector terms, respectively. $\rho(r)$ is the nuclear matter density normalized to A and $\delta\rho(r)$ is the corresponding neutron-proton density difference simply taken as

$$\delta\rho(r)=\frac{N-Z}{A}\rho(r) .$$

p_1 and p_2 are kinematic factors which arise from the transformation from the pion-nucleon center of mass to the pion-nucleus center of mass system. K_F is the Fermi momentum, ω is the total energy of the pion in the center of mass system, and q_π is the charge of the pion.

The nuclear matter density was taken to be a modified harmonic oscillator with radius parameter a and parameter α. The charge distribution was assumed to be uniform with a radius $R_c=[5/3\langle r^2\rangle]^{1/2}$. The density parameters for ^{12}C were taken to be the same as those used by Stricker *et al.*[7] ($a=1.57$ fm, $\alpha=1.33$, and $\langle r^2\rangle^{1/2}=2.46$ fm). The density parameters for ^{14}C were taken from the electron scattering of Kline *et al.*[13] ($a=1.65$ fm, $\alpha=1.38$, and $\langle r^2\rangle^{1/2}=2.56$ fm). The matter density radius parameters were corrected for finite proton size by subtracting the proton radius in quadrature, and for finite meson size by adding the meson radius in quadrature.

The MSU potential parameters were taken to be the published values, set E.[8] The agreement between the calculations and the experimental distributions is rather good for both the $^{14}C(\pi^{\pm},\pi^{\pm})^{14}C$ data as shown in Fig. 3(a), and for the $^{12}C(\pi^{\pm},\pi^{\pm})^{12}C$ data as shown in Fig. 3(b).

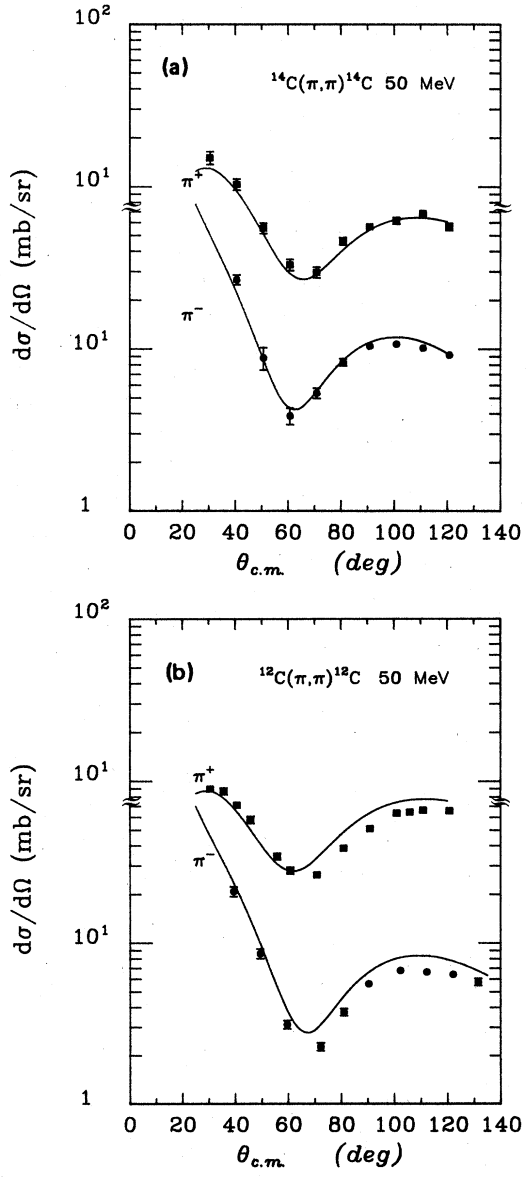

FIG. 3. Elastic differential cross section for (a) $^{14}C(\pi^{\pm},\pi^{\pm})^{14}C$ and (b) $^{12}C(\pi^{\pm},\pi^{\pm})^{12}C$. Curves are calculations with the MSU optical potential, as discussed in the text.

The difference between the calculations for ^{14}C and ^{12}C is due to the isospin terms which involve the nonvanishing $\delta\rho$ term, which was simply taken to be $[(N-Z)/A]\rho(r)$. The agreement between the data and calculations indicates that the simple MSU prescription for the isospin dependence is an effective approximation.

IV. CONCLUSION

The isospin dependence of pion-nucleus elastic scattering has been observed by comparing ^{14}C and ^{12}C differential cross sections at 50 MeV. The cross sections show an effect of the p-wave interaction due to the two excess neutrons even at this low energy for π^- scattering on ^{14}C. The $\pi^- + ^{14}C$ cross section is a factor of 2 larger than for ^{12}C at backward angles. The experimental angular distributions have been analyzed using the MSU optical potential which includes second order effects. This potential describes the experimental angular distribution for ^{14}C ($N \neq Z$) and for ^{12}C ($N = Z$) very well. While the simple $[(N-Z)/A]\rho(r)$ terms in the potential describe the observed isospin dependence, it is surprising that such an approximation works so well. Better understanding of this effect may come from single and double charge exchange experiments, and from elastic scattering from isotopes in different mass regions.

ACKNOWLEDGMENTS

The authors would like to thank the staff of LAMPF for their support during the experiments. We would also like to thank J. A. Carr, K. Stricker, and H. McManus for providing us with their optical model code, and E. Siciliano and F. Myhrer for discussions. This work was supported by the National Science Foundation (University of South Carolina, V.P.I. and SU, and University of Maryland), by the Department of Energy (LANL), and by the Union Carbide Corporation under Contract W-7405-eng-26 with the Department of Energy (ORNL).

*Present address: Department of Physics, Arizona State University, Tempe, AZ 85287.

[1]D. J. Malbrough *et al.*, Phys. Rev. C **17**, 1395 (1978); M. A. Moinester *et al.*, *ibid.* **18**, 2678 (1978); M. Blecher *et al.*, *ibid.* **20**, 1884 (1979); S. H. Dam *et al.*, *ibid.* **25**, 2574 (1982); S. A. Dytman *et al.*, *ibid.* **18**, 2316 (1978); **19**, 971 (1979); R. R. Johnson *et al.*, Nucl. Phys. **A296**, 444 (1978); Phys. Rev. Lett. **43**, 844 (1979); S. A. Dytman *et al.*, *ibid.* **38**, 1059 (1977); J. F. Amann *et al.*, *ibid.* **35**, 426 (1975); F. E. Obenshain *et al.*, Phys. Rev. C **27**, 2753 (1983).

[2]B. M. Preedom *et al.*, Phys. Rev. C **23**, 1134 (1981).

[3]M. J. Leitch *et al.*, Phys. Rev. C **29**, 561 (1984).

[4]B. M. Preedom, in *Proceedings of the Seventh International Conference on High Energy Physics and Nuclear Structure,* edited by M. P. Locher (Birkhauser, Basel, 1977), p. 119; R. P. Redwine, in *Meson-Nuclear Physics—1979 (Houston),* Proceedings of the 2nd International Topical Conference on Meson-Nuclear Physics, AIP Conf. Proc. No. 54, edited by E. V. Hungerford III (AIP, New York, 1979), p. 501; C. H. Q. Ingram, Nucl. Phys. **A374**, 319C (1982).

[5]M. Blecher *et al.*, Phys. Rev. C **28**, 2033 (1983).

[6]R. J. Sobie *et al.*, Phys. Rev. C **30**, 1612 (1984).

[7]K. Stricker, H. McManus, and J. A. Carr, Phys. Rev. C **19**, 929 (1979); K. Stricker, J. A. Carr, and H. McManus, *ibid.* **20**, 2043 (1980).

[8]J. A. Carr, H. McManus, and K. Stricker-Bauer, Phys. Rev. C **25**, 952 (1982).

[9]M. Blecher *et al.*, Phys. Rev. C **25**, 2554 (1982); C. S. Mishra, Master's thesis, University of South Carolina, 1982 (unpublished).

[10]H. Baer, private communication.

[11]E. A. Wadlinger, Nucl. Instrum. Methods **134**, 243 (1976).

[12]P. Y. Bertin *et al.*, Nucl. Phys. **B106**, 341 (1976).

[13]F. J. Kline *et al.*, Nucl. Phys. **A209**, 381 (1973).